# Crystal Structure and Magnetic Properties of Polybis(formamide)bis(μ-formato)cobalt(II): An Extended Two-Dimensional Square Lattice Material Which Exhibits Spontaneous Magnetization below 9 K

**Steven J. Rettig, Robert C. Thompson,* James Trotter, and Shihua Xia**

Department of Chemistry, University of British Columbia, Vancouver, BC, Canada V6T 1Z1

*Received June 29, 1998*

## Introduction

Metal carboxylate complexes have been the subject of study for many years.[1,2] Interest in transition metal complexes has focused on both structure and magnetism, carboxylate ligands tending to bridge metal centers to form oligo- and polymetallic systems which typically exhibit antiferromagnetic exchange effects. For example, the diaqua complex of manganese(II) formate, $[Mn(H_2O)_2(HCO_2)_2]_x$, which is isomorphous and isostructural with the corresponding nickel, cobalt, copper, zinc, iron, and cadmium formates,[3] has a three-dimensional polymeric structure involving bridging formate ions which mediate antiferromagnetic exchange between the metal centers.[4] We report here the synthesis, structure and magnetic properties of the stoichiometrically related complex, $[Co(HCONH_2)_2(HCO_2)_2]_x$, a compound in which cobalt ions are bridged by formate ions in an extended two-dimensional, square lattice, array and in which magnetic studies reveal a spontaneous magnetization at low temperatures. There has been considerable interest in recent years in such materials which are of potential use in information storage applications.[5]

## Experimental Section

**Physical Measurements**. Thermogravimetric analysis (TGA) involved use of a TA Instruments TA 2000 system with a TGA 51 unit. C, H, and N analyses were performed by P. Borda at UBC.

Variable temperature magnetic susceptibilities were measured over the temperature range 2.0−80 K at applied fields of 2549, 5251, 7501, and 9225 G using a vibrating sample magnetometer and methods described previously.[6] A Quantum Design (MPMS) SQUID magnetometer was used to measure susceptibilities over the temperature range 2−300 K at an applied field of 50 000 G and to measure magnetization versus applied field behavior (2−20 K) at fields ranging from 0 to 55 000 G. The sample holder and procedures involving the operation of the SQUID equipment were described previously.[7] Experimental susceptibility data were corrected for the diamagnetism of all atoms ($-72 \times 10^{-6}$ cm$^3$ mol$^{-1}$). All magnetic data reported here were obtained on macroscopic crystals (obtained as described below) which had been ground to a fine powder.

**Table 1.** Crystallographic Data[a]

| | |
|---|---|
| compd | $[Co(HCONH_2)_2(HCO_2)_2]_x$ |
| formula | $C_4H_8CoN_2O_6$ |
| fw | 239.05 |
| cryst syst | monoclinic |
| space group | *C*2/*c* (No. 15) |
| *a*, Å | 12.772(1) |
| *b*, Å | 8.354(1) |
| *c*, Å | 8.243(1) |
| *β*, deg | 93.19(1) |
| *V*, Å$^3$ | 878.2(2) |
| Z | 4 |
| $\rho_{calc}$, g/cm$^3$ | 1.808 |
| *T*, °C | 21 |
| radiation | Mo |
| $\mu$, cm$^{-1}$ | 19.57 |
| *R*(*F*) | 0.030 |
| $R_w(F)$ | 0.031 |

[a] $R = \Sigma||F_o| - |F_c||/\Sigma|F_o|$, $R_w = (\Sigma w(|F_o| - |F_c|)^2/\Sigma w|F_o|^2)^{1/2}$.

**Synthesis and Characterization.** Methylethylphosphinic acid (1.30 g) was mixed with cobalt acetate tetrahydrate (1.00 g) in acetone (75 mL). Stirring the mixture resulted in the formation of a blue solution after 1 h. On addition of 10 mL of formamide the color changed to red, and on standing for three months the solution yielded pink macroscopic crystals of the title compound. Anal. Calcd for $C_4H_8N_2O_6$-Co: C, 20.10; H, 3.37; N, 11.72. Found: C, 20.22; H, 3.37; N, 11.62. Thermal analysis (TGA): complete loss of formamide over the temperature range 157−233 °C with further decomposition above 276 °C. Later work showed the compound can be obtained more conveniently as a microcrystalline powder. To a mixture of 4.0 mL of formic acid and 10 mL of formamide was added cobalt perchlorate hexahydrate (0.732 g) in 50 mL of acetone. The solution was stirred and a pink precipitate formed after 3 days. The product was washed with acetone and dried in vacuo at room temperature (yield 87%). Anal. Found: C, 19.99; H, 3.40; N, 11.24. An X-ray powder diffractogram recorded in the range $2\theta = 4-60°$ on a Rigaku rotating anode powder X-ray diffractometer using Cu Kα radiation confirmed that this microcrystalline sample and the macroscopic crystals are the same.

**X-ray Crystallographic Analysis of $[Co(HCONH_2)_2(HCO_2)_2]_x$.** Crystallographic data appear in Table 1. The final unit-cell parameters were obtained by least-squares on the setting angles for 25 reflections with $2\theta = 20.6-31.8°$. The intensities of three standard reflections, measured every 200 reflections throughout the data collection, showed only small random fluctuations. The data were processed[8] and corrected for Lorentz and polarization effects and for absorption (empirical, based on azimuthal scans, relative transmission factors 0.78−1.00).

The structure analysis was initiated in the centrosymmetric space group *C*2/*c* on the basis of the *E* statistics, this choice being validated by subsequent calculations. The structure was solved by direct methods. The Co atom lies on a center of symmetry. The $NH_2$ group of the $HCONH_2$ ligand was modeled as 4-fold disordered (52:19:17:12). The population parameters were adjusted as the refinement progressed to yield roughly equal thermal parameters for the four components of the disordered nitrogen atom. All non-hydrogen atoms except N(1c) were refined with anisotropic thermal parameters. The hydrogen atoms were fixed in calculated positions with C−H = 0.98 Å, N−H = 0.97−0.98 Å, and $B_H = 1.2B_{bonded\ atom}$. The hydrogen atoms associated with the 12% occupancy $HCONH_2$ ligand were not included in the model. A secondary extinction correction was applied (Zachariasen type, isotropic), the final value of the extinction coefficient was $8.3(2) \times 10^{-6}$. Neutral atom scattering factors for all atoms and anomalous dispersion corrections for the non-hydrogen atoms were taken from the *Interna-*

* To whom enquiries may be addressed. Telephone: (604) 822-4979. Fax: (604) 822-2847. E-mail: thompson@chem.ubc.ca.

(1) Oldham, C. In *Prog. Inorg. Chem.* **1968**, *10*, 223.
(2) Doedens, R. J. In *Prog. Inorg. Chem.* **1976**, *21*, 209.
(3) Kaufman, A.; Afshar, C.; Rossi, M.; Zacharias, D. E.; Glusker, J. P. *Struct. Chem.* **1993**, *4*, 191.
(4) Wagner, G. R.; Friedberg, S. A. *Phys. Lett.* **1964**, *9*, 11.
(5) Kahn, O. *Adv. Inorg. Chem.* **1995**, *43*, 179.
(6) Haynes, J. S.; Oliver, K. W.; Rettig, S. J.; Thompson, R. C.; Trotter, J. *Can. J. Chem.* **1984**, *62*, 891.
(7) Ehlert, M. K.; Rettig, S. J.; Storr, A.; Thompson, R. C.; Trotter, J. *Can. J. Chem.* **1989**, *67*, 1970.
(8) *teXsan: Crystal structure analysis package*; Molecular Structure Corp.: The Woodlands, TX, 1995.

10.1021/ic980742h CCC: $18.00 
Published on Web 02/25/1999

**Table 2.** Selected Bond Lengths (Å) and Angles (deg) for $[Co(HCONH_2)_2(HCO_2)_2]_x$[a]

| | | | |
|---|---|---|---|
| Co(1)−O(1) | 2.082(1) | Co(1)−O(2)[b] | 2.085(1) |
| Co(1)−O(3) | 2.122(2) | O(1)−C(1) | 1.242(2) |
| O(2)−C(1) | 1.242(2) | O(3)−C(2) | 1.224(3) |
| N(1)−C(2) | 1.225(6) | | |
| O(1)−Co(1)−O(1)[a] | 180.0 | O(1)−Co(1)−O(2)[b] | 92.74(5) |
| O(1)−Co(1)−O(2)[c] | 87.26(5) | O(1)−Co(1)−O(3) | 90.97(7) |
| O(1)−Co(1)−O(3)[a] | 89.03(7) | O(2)[b]−Co(1)−O(2)[c] | 180.0 |
| O(2)[b]−Co(1)−O(3) | 91.57(6) | O(2)[b]−Co(1)−O(3)[a] | 88.43(6) |
| O(3)−Co(1)−O(3)[a] | 180.0 | Co(1)−O(1)−C(1) | 124.6(1) |
| Co(1)[d]−O(2)−C(1) | 123.6(1) | Co(1)−O(3)−C(2) | 123.7(2) |
| O(1)−C(1)−O(2) | 125.1(2) | O(3)−C(2)−N(1) | 132.6(4) |

[a] Roman superscripts refer to symmetry operations: (a) $^1/_2 - x$, $^1/_2 - y$, $1 - z$; (b) $^1/_2 - x$, $-^1/_2 + y$, $^1/_2 - z$; (c) $x$, $1 - y$, $^1/_2 + z$; (d) $x$, $1 - y$, $-^1/_2 + z$.

*tional Tables for X-ray Crystallography*.[9] Selected bond lengths and bond angles appear in Table 2. A complete table of crystallographic data, final atomic coordinates and equivalent isotropic thermal parameters, anisotropic thermal parameters, complete tables of bond lengths and angles, torsion angles, intermolecular contacts, and hydrogen bond parameters are included as Supporting Information.

## Results and Discussion

**Synthesis and Structure of $[Co(HCONH_2)_2(HCO_2)_2]_x$.** Our initial synthesis of the title compound was serendipitous. We were attempting to obtain the phosphinate compound $Co(HCONH_2)_2[(CH_3)(C_2H_5)PO_2]_2$ in crystalline form. In the process the intended product did not materialize; instead, slow hydrolysis of formamide generated formate ions and crystals of $[Co(HCONH_2)_2(HCO_2)_2]_x$ suitable for single-crystal X-ray diffraction studies. The process involved in this synthesis has been described before in the synthesis of some copper(II) formate derivatives.[10,11] We subsequently obtained the title compound by rational synthesis involving direct reaction between cobalt ions, formic acid, and formamide. This latter route yields only microcrystalline powder. A key factor in obtaining macroscopic crystals appears to be the slow generation of the anion by hydrolysis.

The atom labeling scheme and a section of the polymeric sheet structure of $[Co(HCONH_2)_2(HCO_2)_2]_x$ are given in Figures 1 and 2, and a portion of the three-dimensional structure is depicted in Figure 3. As seen in Figure 1 the nitrogen atoms are disordered; for clarity only N(1) is shown in Figures 2 and 3. Each cobalt ion is linked to four other cobalt ions by four formate ligands, adopting the anti-anti configuration. This generates a square lattice extended sheet structure. The O-bonded, trans-coordinated formamide ligands complete the octahedral coordination sphere of each cobalt ion. Hydrogen bonds between formamide molecules and formate anions link the sheets together, generating a three-dimensional lattice.

**Magnetic Properties.** Magnetic moment and magnetic susceptibility versus temperature plots are shown for four values of applied magnetic field in Figure 4. The moment decreases with temperature to 9 K at which point there is an abrupt increase to a maximum value before decreasing with decreasing

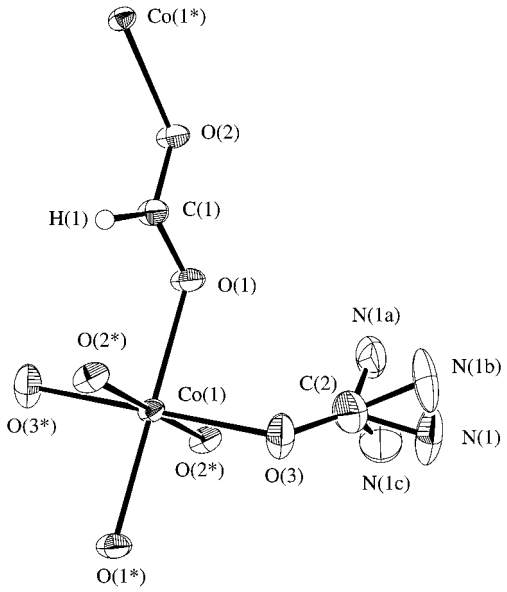


**Figure 1.** Molecular structure of the repeat unit and atom numbering scheme; 33% probability thermal ellipsoids are shown.

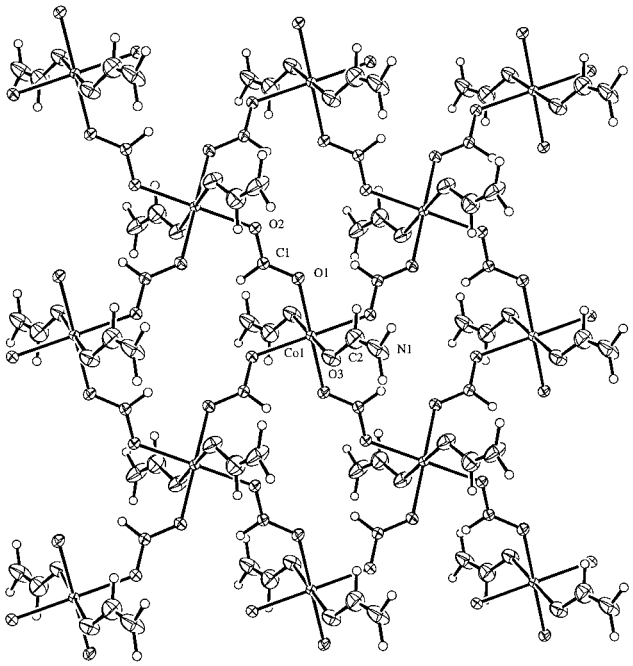


**Figure 2.** Section of the polymeric sheet structure; 33% probability thermal ellipsoids are shown.

temperature in the lowest temperature region. At temperatures above 9 K the compound shows antiferromagnetic behavior. This is clearly seen in the magnetic susceptibility plot (Figure 4) which shows an incipient maximum in the 9−18 K region. The anomaly at 9 K which corresponds to an abrupt increase in the moment and below which the susceptibility becomes field dependent suggests a ferromagnetic transition. Further support for this comes from magnetization versus applied field plots at five different temperatures (Figure 5). At temperatures above 9 K the plots are linear and extrapolate to zero magnetization at zero applied field. Below this temperature the plots are not linear and extrapolate to yield net magnetization at zero applied field. The highest magnetization reached at 2 K and 55 000 G is 3710 $cm^3$ G $mol^{-1}$, significantly below the theoretical saturation magnetization of 16 755 $cm^3$ G $mol^{-1}$.[12] Cycling the applied field between +55 000 and −55 000 G at 4.8 K generates a

(9) *International Tables for X-ray Crystallography*; Kynoch Press: Birmingham, U.K. 1974; Vol. IV, pp 99−102. (b) *International Tables for Crystallography*; Kluwer Academic Publishers: Boston, MA, 1992; pp 200−206.
(10) Nifontova, G. A.; Filipenko, O. S.; Astokhova, A. S.; Lavrent'ev, I. P.; Atovmyan, L. O. *Koord. Khim.* **1990**, *16*, 218; *Coord. Chem. (Engl. Trans)* **1990**, *16*, 121.
(11) Chulkevich, A. K.; Lavrent'ev, I. P.; Moravskii, A. P.; Khidekel', M. L.; Ponomarev, V. I.; Filipenko, O. S.; Atovmyan, L. O. *Koord. Khim.* **1986**, *12*, 470. *Coord. Chem. (Engl. Trans)* **1986**, *12*, 285.

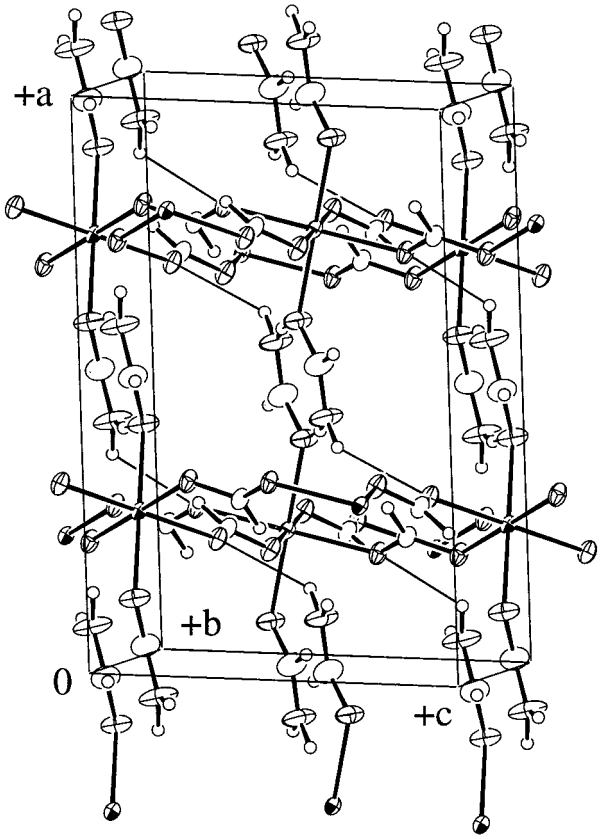


**Figure 3.** Portion of the three-dimensional network; 33% probability thermal ellipsoids are shown.

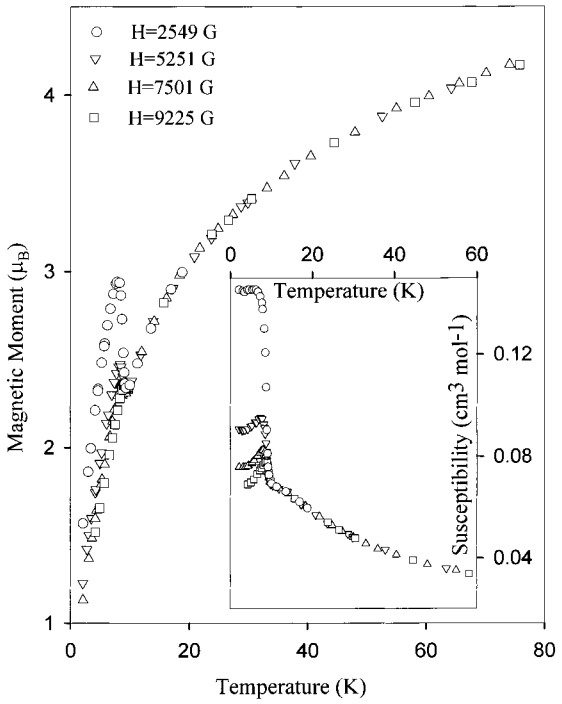


**Figure 4.** Plot of magnetic moment and magnetic susceptibility versus temperature at four values of applied field.

hysteresis loop as shown in Figure 6. From this is obtained a coersive field of 1800 G and a remnant magnetization of 350 $cm^3$ G $mol^{-1}$.

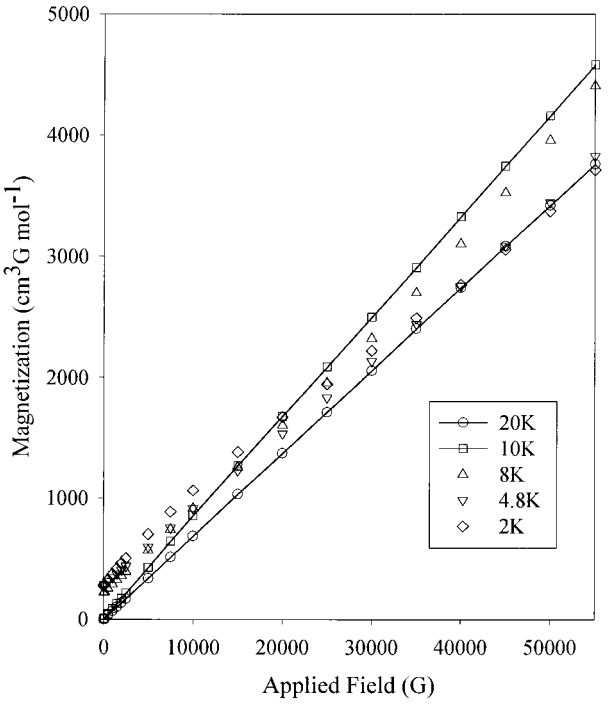


**Figure 5.** Plot of magnetization versus applied field at five temperatures.

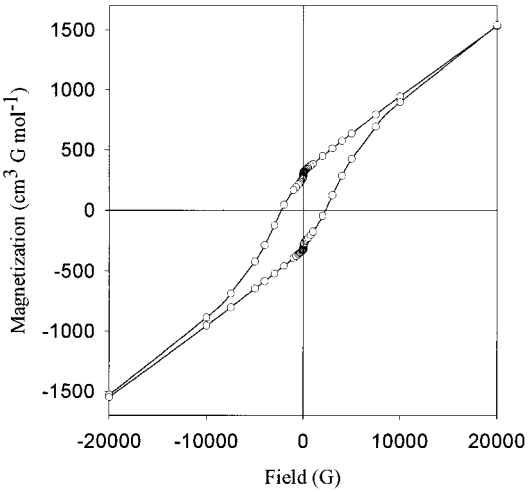


**Figure 6.** Field dependence of magnetization at 4.8 K.

We interpret the magnetic properties as a consequence of canted spin antiferromagnetism leading to weak ferromagnetism at low temperatures.[13] In the high-temperature region, antiferromagnetic coupling between metal centers via formate ligands within the extended two-dimensional sheets leads to a canted spin structure. Below 9 K three-dimensional magnetic ordering of the uncompensated spins occurs. A mechanism for this could involve interactions via the H-bonding network linking the sheets. A canted spin structure is supported by the fact the magnetization falls considerably short of the theoretical saturation value. In addition, the X-ray structure shows a feature characteristic of such systems, that of a systematic alternation of the relative orientation of neighboring metal chromophores.[14] As a measure of this the dihedral angle between the O(1)−Co−O(1*) vectors on adjacent cobalt ions is 52.40(8)°.

(12) Carlin, R. L. *Magnetochemistry*; Springer-Verlag: Berlin, 1986; pp 7−9.

(13) Kahn, O. *Molecular Magnetism*; VCH Publishers: New York, 1993; p 322.

(14) Rettig, S. J.; Storr, A.; Summers, D. A.; Thompson, R. C.; Trotter, J. *J. Am. Chem. Soc.* **1997**, *119*, 8675.

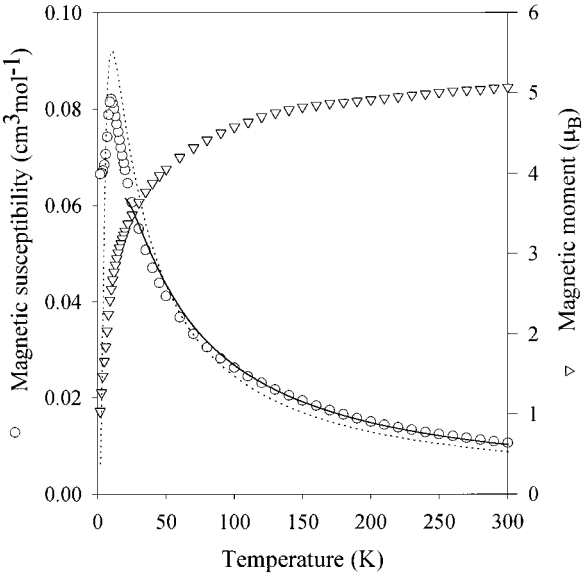


**Figure 7.** Plot of magnetic moment and magnetic susceptibility versus temperature at 50 000 G. Lines calculated from theory as described in the text.

That applied fields may significantly affect magnetic ordering is clearly shown in Figure 4. As the applied field is increased from 2550 to 9225 G the magnetic moment anomaly at 9 K virtually disappears due to disruption of the interlayer exchange. Susceptibility and moment versus temperature plots at 50 000 G (Figure 7) reveal no magnetic anomaly. At this applied field the interlayer exchange appears to be destroyed. However, the intralayer exchange is still present; the susceptibility passes through a maximum at 10 K, behavior typical of a system showing antiferromagnetic exchange coupling. At the lowest temperatures the susceptibilities tend toward a constant value, a consequence presumably of spin canting leading to residual spin within the sheets. The dotted line in Figure 7 is the susceptibility calculated using Lines' expression for a square lattice 2-D array of $S = {}^3/_2$ ions with $g = 2.43$ and $J = 1.8$ cm$^{-1}$.[15] The fact that there is only qualitative agreement between the lines calculated from theory[16] and experiment is not surprising. Octahedral cobalt (II) has an orbitally degenerate ground electronic state and single-ion spin−orbit coupling results in temperature-dependent moments.[17] This effect is not accommodated by the theory which allows for orbital contributions only by permitting $g$ to differ from the free-ion value. In addition, the Lines model is not quantitative below $kT \sim 3.4J$[15] and, in any event, does not accommodate the effects of spin canting. Since these latter effects are most pronounced at low temperatures we examined fits to the data in the higher temperature regions. An example of this is given in Figure 7 where the fit was to data at 20 K and above only. The calculated susceptibilities, represented by the solid line, were obtained with $J = 3.3$ cm$^{-1}$ and $g = 2.68$. While agreement between theory and experiment is improved, the unrealistically high $g$ value points to the inadequacies of the model in accommodating the orbital angular momentum contribution to the susceptibility. Unfortunately no solution exists for a 2-D Ising model applicable to $S = {}^3/_2$, preventing further analysis of these data.

Structurally and magnetically, our observations on $[Co(HCONH_2)_2(HCO_2)_2]_x$ parallel those reported earlier for [Fe(4-imidazoleacetate)$_2$]·2CH$_3$OH.[18] In the latter compound antiferromagnetic coupling within sheets of octahedral iron centers leads to a canted spin structure. Hydrogen-bonding interactions between sheets are presumed to promote interactions between the residual spins on the sheets resulting in the observed spontaneous magnetization below 15 K. The material shows hysteresis behavior at 4.2 K with a coersive field of 6200 G and remnant magnetization of 1200 cm$^3$ G mol$^{-1}$.

The present study illustrates how a ligand such as formate, which is capable of mediating antiferromagnetic exchange between metal centers, can generate residual spin on metal centers in materials where structural factors lead to spin canting. In favorable cases, as found here, interactions between the residual spins can lead to long-range three-dimensional magnetic ordering and spontaneous magnetization at low temperatures. It is important to note that both here and in the case of the related compound, [Fe(4-imidazoleacetate)$_2$]·2CH$_3$OH,[18] the interaction between the layers appears to involve hydrogen bonds.

In studies on the stoichiometrically related compound, $[Co(H_2O)_2(HCO_2)_2]_x$, at fields of 2549, 5251, and 7501 G, we found magnetic moment versus temperature behavior that was very similar to that observed for the title compound. In this instance the ferromagnetic anomaly occurs at 8 K. This aqua derivative has a complex three-dimensional covalent lattice structure[3] and is probably another example of a material exhibiting spin canting.

**Acknowledgment.** The Natural Sciences and Engineering Research Council of Canada is thanked for financial support.

**Supporting Information Available:** Tables of crystallographic data, non-H atom coordinates, bond lengths, and bond angles, hydrogen atom coordinates, anisotropic thermal parameters for non-H atoms, bond lengths and angles involving hydrogen, torsion angles, nonbonded contacts, and hydrogen bonds for the compound. This material is available free of charge via the Internet at http://pubs.acs.org.

IC980742H

(15) Lines, M. E. *J. Phys. Chem. Solids* **1970**, *31*, 101.
(16) The function minimized in the least-squares fitting procedure is given in a recent publication.[14]
(17) Figgis, B. N.; Gerloch, M.; Lewis, J.; Mabbs, F. E.; Webb, G. A. *J. Chem. Soc. (A)* **1968**, 2086.
(18) Martinez-Lorente, M. A.; Petrouleas, V.; Poinsot, R.; Tuchagues, J. P.; Savariault, J. M.; Drillon, M. *Inorg. Chem.* **1991**, *30*, 3587.